Hyperspectral Image Classification Based on Local Binary Patterns and PCANet

Huizhen Yang[a], Feng Gao[a], Junyu Dong[a], Yang Yang[b]
[a]Ocean University of China, Department of Computer Science and Technology
[b]Ocean University of China, Law & Politics School

ABSTRACT

Hyperspectral image classification has been well acknowledged as one of the challenging tasks of hyperspectral data processing. In this paper, we propose a novel hyperspectral image classification framework based on local binary pattern (LBP) features and PCANet. In the proposed method, linear prediction error (LPE) is first employed to select a subset of informative bands, and LBP is utilized to extract texture features. Then, spectral and texture features are stacked into a high dimensional vectors. Next, the extracted features of a specified position are transformed to a 2-D image. The obtained images of all pixels are fed into PCANet for classification. Experimental results on real hyperspectral dataset demonstrate the effectiveness of the proposed method.

Keywords: local binary patterns, hyperspectral image, pattern classification, principal component analysis, convolutional network.

1. INTRODUCTION

With the development of remote sensing technology, hyperspectral images with high spatial resolution are easy to obtain in our daily life. Over the past two decades, hyperspectral images have been widely applied in the field of urban land cover monitoring [1], vegetation classification [2], environmental monitoring [3], agricultural exploration [4], etc. Hyperspectral sensor provides hundreds of narrow spectral channels from the same area on the surface of the earth. The detailed spectral information increases the capability of distinguishing between different land-cover classes with promoting accuracy. In this paper, we mainly focus on the problem of land-cover classification by using hyperspectral images.

In the early studies of hyperspectral image classification, researchers only used the spectral information [5-7]. Camps-Valls et al. [5] proposed a kernel-based method for hyperspectral image classification. In the method, regularized radial basis function neural networks are introduced to improve the classification performance. Demir and Erturk [8] proposed a hyperspectral image classification method based on relevance vector machines. The method is of high computational efficiency and more suitable for real-time classification applications. Later, some researchers recognized that the combination of spectral and spatial information could provide better performance. Therefore, many classification methods based on spectral-spectral features are proposed. In [9], a method based on extended morphological profile was proposed for fusion of the spatial and spectral information. Li et al. [10] used Gabor feature for hyperspectral image spatial information analysis.

Recently, deep learning methods have displayed promising performance for hyperspectral image classification. In [11], deep belief network was applied in hyperspectral image classification. Chen et al. [12] employed a stacked autoencoder to extract features of hyperspectral image. In [13], convolutional autoencoder was utilized to learn representative features from hyperspectral image. However, as mentioned in [14], deep learning-based methods might perform poor when the number of training samples is small. Chan et al. [15] proposed a simplified deep learning method called PCANet. It is only comprised of two convolutional layers and one feature generation layer. Although the architecture of PCANet is rather simple, it can achieve competitive results against many state-of-the-art deep learning models in many classification tasks.

In this paper, we propose a novel hyperspectral image classification framework based on LBP features and PCANet. In the proposed method, linear prediction error (LPE) [16] is first employed to select a subset of informative spectral bands, and LBP is utilized to extract texture features. Then, spectral and texture features are stacked into a high dimensional vectors. Next, the extracted features of a specified position are transformed to a 2-D image. The obtained images

of all pixels are fed into PCANet for classification. Experimental results on real hyperspectral dataset demonstrate the effectiveness of the proposed method.

The remainder of this paper is organized as follows. In Section 2, we present the classification framework of the proposed method. Section 3 shows the experimental results and discussions. Finally, Section 4 draws conclusion of the proposed method. Some hints for plausible future research are also provided.

2. METHODOLOGY

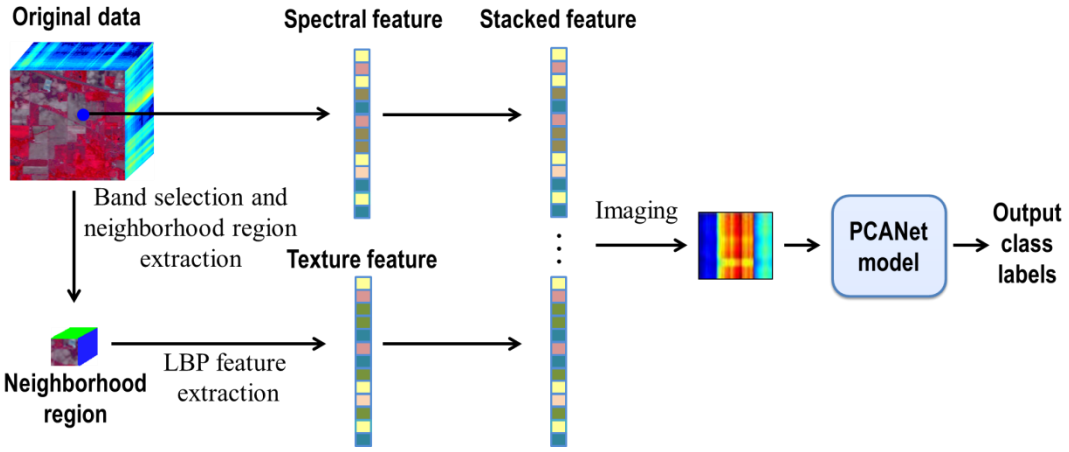

Figure 1 The framework of the proposed method.

In this section, the detailed implementation of the proposed method is described. The overall framework of the proposed method is illustrated in Fig. 1. To be specific, the proposed hyperspectral classification method is comprised of two main steps:

Step 1 — Extraction of the spectral and texture features. In the spectral feature extraction, we use all the spectral channels as input. In the texture feature extraction, LPE [16] is utilized to select a subset of informative spectral bands, and LBP [17] is employed to extract texture features. Then, spectral and texture features are stacked into high dimensional vectors.

Step 2 — Integrating the texture and spectral features into PCANet for classification. The extracted spectral and texture features for each pixel are transformed from a 1-D vector to a 2-D image. Then, the obtained images are fed into PCANet for classification.

2.1 Extraction of the texture and spectral features

Feature extraction in the proposed method is consisted of two parallel modules: spectral feature extraction and texture feature extraction. In the spectral feature extraction, all the spectral channels are used as input, as shown in Fig. 1.

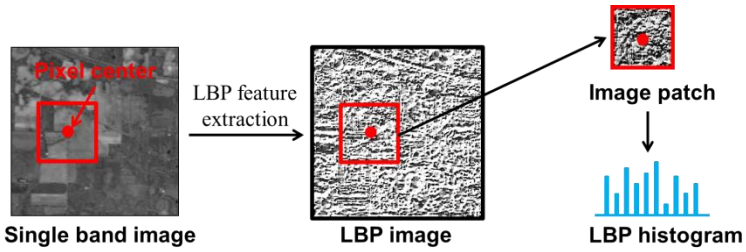

Figure 2 Implementation of LBP feature extraction.

In texture feature extraction, if all the spectral channels are used in the texture feature extraction, the complexity of texture feature extraction will increase the computational burden. Therefore, we select informative bands to reduce the computational complexity before extracting texture feature. In this paper, LPE [16] is utilized to select the most distinc-

tive and informative bands. LPE is a simple but effective band selection method, and based on band similarity measurement. Specifically, the basic steps of LPE can be summarized as follows: First, choose a pair of bands B_1 and B_2, and the resulting selected band subset is $F = \{B_1, B_2\}$. Second, find a third band B_3 that is the most similar to all the bands in the current F.

Then, the selected band subset will be updated as $F = F \cup \{B_3\}$. Finally, continue the second step until we obtain enough bands. In LPE, the employed similarity criteria is linear prediction. In our implementations, we select 7 bands for texture feature extraction.

After band selection, LBP operator which describes the edges, lines, and flat areas of the texture information, is utilized to each selected band. Given a center pixel t_c, each neighbor pixels of a local region is assigned with a binary label, which is either "1" or "0". To be specific, the k neighboring pixels are generated from a circle of radius r centered at t_c. The LBP code for the center pixel t_c can defined as:

$$\mathrm{LBP}_{k,r}(t_c) = \sum_{i=1}^{k-1} U(t_i - t_c)2^i, \tag{2}$$

where $U(t_i - t_c) = 0$ if $t_i \le t_c$, and $U(t_i - t_c) = 1$ if $t_i > t_c$. The LBP code presents the texture information in a local region. After obtaining the LBP codes of all the pixels, a histogram will be computed over a local patch centered at the interested pixel, as illustrated in Fig. 2. All bands of LBP histograms are concatenated to form the texture feature vector.

2.2 Integrating the texture and spectral features into PCANet for classification

The spectral features contain crucial information for discriminating different kinds of ground categories. The texture features decrease the intra-class variance, and then can improve the classification performance. The integration of spectral and texture features provides significant performance improvements, it is addressed by vector stacking, as shown in Fig. 1. Next, the stacked features are "imaging" to an image. Here imaging refers to transform from a 1-D vector to a 2-D image. Supposing that v_i is the stacked feature vector of a pixel, and then the imaging process is denoted by:

$$v_i \to \mathbf{V}_i \in R^{k' \times k}, \tag{2}$$

In this paper, the width and height of the imaging results are set the same for simplifying. Next, the imaging results are fed into PCANet for classification.

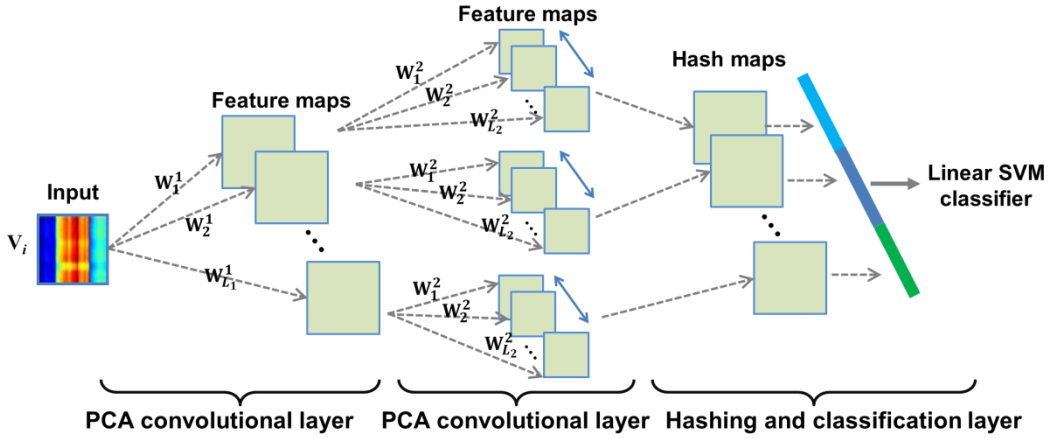

Figure 3 Flowchart of PCANet.

PCANet is a simplified deep learning framework, which is comprised of PCA and binary hashing. Its process is divided into three layers: the first and second are PCA convolutional layers, the third is hashing and classification layer, as shown in Fig. 3.

In the first layer, supposing that $\mathbf{V}_i$ is an input sample image. PCANet first takes a $k_1 \times k_2$ patch around each pixel, and collects all the vectorized patches to form a matrix $\mathbf{X}_i \in \mathbb{R}^{k_1 k_2 \times n}$. Here n is the number of patches extracted from $\mathbf{V}_i$. Next, we construct a matrix for each input image and combine them together:

$$\mathbf{X} = [\mathbf{X}_1, \mathbf{X}_2, \ldots, \mathbf{X}_N] \in \mathbb{R}^{k_1 k_2 \times Nn}, \tag{2}$$

where N is the number of input images. PCA is utilized to minimize the reconstruction error within a family of orthonormal filters. The filters are expressed as:

$$\mathbf{W}_l^1 = \mathrm{mat}_{k_1 k_2}(q_l(\mathbf{X}\mathbf{X}^T)) \in \mathbb{R}^{k_1 \times k_2}, \ l = 1, 2, \ldots, L_1, \tag{2}$$

where $\mathrm{mat}_{k_1 k_2}(\cdot)$ is a function that reshapes a vector to a matrix, and $q_l(\mathbf{X}\mathbf{X}^T)$ represents the principle vector of $\mathbf{X}\mathbf{X}^T$. L_1 corresponds to the number of filters in the first layer. Therefore, the output of the first layer can be obtained by

$$\mathbf{V}_i^l = \mathbf{V}_i * \mathbf{W}_l^1, \ i = 1, 2, \ldots, N. \tag{2}$$

Then we conduct the same process as that of the first layer for all the $\mathbf{V}_i^l$, the output of the second layer is obtained. Assuming that the number of filters in the second layer is L_2, we would obtain $L_1 L_2$ images.

In the final layer of PCANet, a binary quantization process is conducted. Specifically, each of the L_1 images is separated into many local blocks. The histogram of each block is computed, and all the histograms are concatenated into one vector. Moreover, SVM classifier is utilized to determine the classification results.

3. EXPERIMENTAL RESULTS AND ANALYSIS

3.1 Dataset description and parameter tuning

In this paper, we test the proposed method and several closely related methods on the Indian Pines dataset. The dataset is acquired in June 1992 by National Aeronautics and Space Administration's Airborne Visible/Infrared Imaging Spectrometer (AVIRIS) sensor at the northwest Indiana's Indian Pine test site. The image scene, with a vegetation-classification scenario of 145 × 145 pixels and 200 spectral bands, contains two-thirds agriculture, and one-third forest or other natural perennial vegetation. In our paper, the ground-truth is designated into 16 classes and the number of total labeled pixels is 10249. The number of training and testing samples is listed in Table 1, respectively.

Table 1 Class label and train-test distribution of samples in the Indian Pines dataset.

#	class	Training	Testing
1	Alfalfa	6	40
2	Corn-notill	30	1398
3	Corn-mintill	30	800
4	Corn	24	213
5	Grass-pasture	30	453
6	Grass-trees	30	700
7	Grass-pasture-mowed	3	25
8	Hay-windrowed	30	448
9	Oats	2	18
10	Soybean-notill	30	942
11	Soybean-mintill	30	2425
12	Soybean-clean	30	563
13	Wheat	22	183
14	Woods	30	1235
15	Build-Grass-Trees-Drives	30	356
16	Stone-Steel-Towers	10	83
	Total	367	9882

In the proposed classification framework, many parameters, such as the quantity of selected bands, (m, r) of the LBP operator and the number and size of filters, the block size of PCANet, are of great significance to the performance of hyperspectral classification. Firstly, LPE is applied to reduce the number of channels before extracting LBP feature. In [18], the number of selecting bands and patch size were fixed to be 7 and 17×17 and it would achieve the best perfor-

mance. Setting parameters in our experiment is same as that. Furthermore, the parameters filter size, filter number and patch size of PCANet are fixed to be (5, 5), (3, 5) and (9, 9). The impacts from different (m, r) are investigated as shown in Table 2.

Table 2 Classification accuracy by varing (m, r) of LBP.

Value of *r*	Value of *m*	Classification accuracy
1	4	91.67
1	8	93.56
1	16	**93.71**
2	4	89.70
2	8	92.90
2	16	93.26

3.2Experimental results

In this subsection, in order to demonstrate the effectiveness of the proposed method, we choose six closely related methods for comparison. These methods include SVM [18], ELM [19], PCANet [15], LBP_SVM, LBP_ELM [20]. For SVM, it is a very popular classifier and widely used in hyperspectral image classification. ELM classifier is considered to be more computational efficient than SVM, and has been recently applied to hyperspectral image classification. LBP_SVM and LBP_ELM are proposed by Li [20]. It is demonstrated that, LBP feature provides good performance. The overall accuracy (OA) and average accuracy (AA) are used to evaluate the classification performance of different methods.

Table 3 Overall classification accuracy (%) and average accuracy (%) by different methods on the Indian Pines dataset.

Class	SVM	ELM	PCANet	LBP_SVM	LBP_ELM	Proposed method
1	80.00	12.50	65.00	**100**	**100**	**100**
2	58.37	53.36	58.58	83.33	84.26	**91.42**
3	57.88	59.88	65.50	97.00	97.13	**98.50**
4	62.20	67.61	74.18	**98.59**	**98.59**	98.12
5	86.34	85.24	85.90	98.68	**98.90**	97.36
6	95.29	97.43	89.86	96.43	98.00	**99.57**
7	68.00	72.00	72.00	**100**	**100**	96.00
8	93.53	98.66	96.88	**100**	**100**	**100**
9	33.33	11.11	50.00	**100**	**100**	**100**
10	59.45	51.91	68.68	84.18	84.39	**87.69**
11	53.20	47.71	55.13	84.29	83.75	**88.91**
12	57.73	71.94	71.76	83.48	84.72	**91.12**
13	98.36	98.91	99.45	**100**	**100**	**100**
14	90.04	89.64	89.47	98.79	99.03	**100**
15	55.62	64.61	64.33	97.47	98.31	**99.16**
16	93.98	87.95	93.98	**97.59**	**97.59**	**97.59**
OA	67.03	66.24	70.71	90.49	90.77	**94.01**
AA	71.71	66.90	75.04	94.99	95.29	**96.59**

In the experiment, we randomly choose the training and testing samples. The performance of each algorithm is compared by OA and AA. The classification accuracy for each class is shown in Table 3. We observe that the classification accuracy of the proposed method for each class is nearly better than the other methods, except for the Corn, Grass-pasture and Grass-pasture-mowed. Especially, the classification results of the proposed method for Hay-windrowed, Oats, Wheat and Woods run up to 100%. The proposed method obtains the best OA and AA values. The quantitative results clearly demonstrate that the LBP is a highly discriminative texture feature for hyperspectral image analysis. In addition, the simple framework of PCANet has some advantage in hyperspectral image classification.

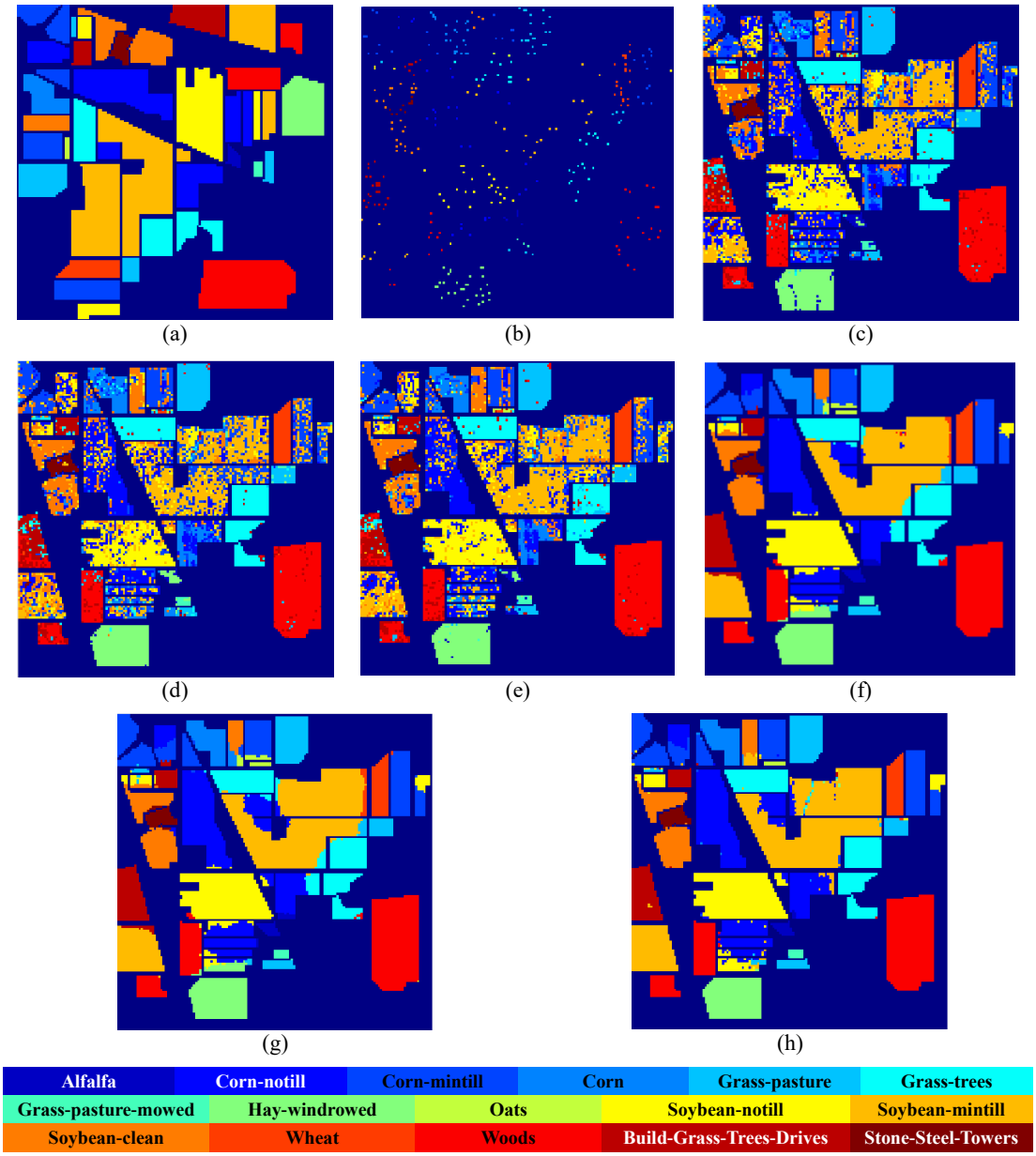

Figure 4 The classificaiton results using 367 tranining samples for the Indian Pines datase with 16 classes. (a) Ground truth; (b) training set; (c) result by SVM; (d) result by ELM; (e) result by PCANet; (f) result by LBP_SVM; (g) result by LBP_ELM; (h) result by the proposed method.

The maps on labeled pixels obtained from the different methods are shown in Fig. 4. These classification results are consistent with the results shown in Tables 3. The ground truth map and training sets are shown in Fig. 4 (a) and (b), respectively. Results obtained by integrating texture and spectral features are less noisy than the results obtained by only spectral features. For example, the classification results of LBP_SVM and LBP_ELM are more accurate than the results of SVM and ELM. In addition, Fig. 4 (e) shows that the result of PCANet is smoother than that of SVM and ELM. In Fig. 4 (h), the combination of LBP feature and deep feature obtains a much smoother classification result than other methods that only use texture or spectral information.

4. CONCLUSION

In this paper, we propose a novel framework for hyperspectral image classification based on LBP and PCANet. Above all, informative spectral bands are selected by using LPE. In our experiment, LBP and PCANet are applied to extract spatial features and deep features, respectively. LBP operator is calculated on the local grid of the image, and maintains a good invariance to the shape and the illumination of the image. PCANet is a simple deep learning network, and consists of cascaded PCA, binary hashing, and block histograms. To improve the classification performance, we combine hand-crafted feature and deep information. Deep features (PCANet) provides as a reasonable solution to make up for the defect of hand-crafted features. The experimental results have demonstrated on the Indian Pines dataset that the proposed method yields good performance, and it gives rise to a better classification result than several closely related methods.

ACKNOELEDGEMENT

The authors would like to thank all the anonymous reviewers for their helpful suggestions. This work was supported by the National Natural Science Foundation of China (No. 41401174, 41606198, 61271405, 61576011, 61401413) and in part by the Shandong Province Natural Science Foundation of China under Grant ZR2016FB02.

REFERENCES

[1] X. Tong, H. Xie, Q. Weng, "Urban land cover classification with airborne hyperspectral data: What features to use?" *IEEE J. Sel. Topics Appl. Earth Observ. Remote Sens.*, **7**, 3998–4009, (2014).

[2] M. Wang et al., "The analysis about factors influencing the supervised classification accuracy for vegetation hyperspectral remote sensing imagery," in *International Congress on Image and Signal Processing*, pp. 1685–1689 (2011).

[3] H. Kalluri et al., "Decision-level fusion of spectral reflactance and derivative information for robust hyperspectral land cover classification," *IEEE Trans. Geosci. Remote Sens.*, **48**, 4047–4058, (2010).

[4] B. Datt et al., "Preprocessing EO-1 hyperion hyperspectral data to support the application of agricultural indexes," *IEEE Trans. Geosci. Remote Sens.*, **41**, 1246–1259, (2003).

[5] G. Camps-Valls, L. Bruzzone, "Kernel-based methods for hyperspectral image classification," *IEEE Trans. Geosci. Remote Sens.*, **43**, 1351–1362, (2005).

[6] G. Camps-Valls et al., "Composite kernels for hyperspectral image classification," *IEEE Geosci. Remote Sens. Lett.*, **3**, 93–97, (2006).

[7] G. Camps-Valls et al., "Semi-supervised graph-based hyperspectral image classification," *IEEE Trans. Geosci. Remote Sens.*, **45**, 3044-3054, (2007).

[8] B. Demir, S. Erturk, "Hyperspectral image classification using relevance vector machines," *IEEE Geosci. Remote Sens. Lett.*, **4**, 586–690, (2007).

[9] M. Fauvel et al., "Spectral and spatial classification of hyperspectral data using SVMs and morphological profiles," *IEEE Trans. Geosci. Remote Sens.*, **46**, 3804–3814, (2008).

[10] W. Li, Q. Du, "Gabor-filtering-based nearest regularized subspace for hyperspectral image classification," *IEEE J. Sel. Topics Appl. Earth Observ. Remote Sens.*, **7**, 1012–1022, (2014).

[11] T. Li, J. Zhang, Y. Zhang, "Classification of hyperspectral image based on deep belief networks," in *IEEE International Conference on Image Processing*, pp. 5132–5136, (2015).

[12] Y. Chen et al., "Deep learning-based classification of hyperspectral data," *IEEE J. Sel. Topics Appl. Earth Observ. Remote Sens.*, **7**, 2094–2107, (2014).

[13] W. Zhao et al., "On combining multiscale deep learning features for the classification of hyperspectral remote sensing imagery," *International Journal of Remote Sensing*, **36**, 3368–3379, (2015).

[14] B. Pan, Z. Shi, X. Xu, "R-VCANet: A new deep-learning-based hyperspectral image classification method," *IEEE J. Sel. Topics Appl. Earth Observ. Remote Sens.*, **10**, 437–449, (2017).

[15] T. H. Chan et al., "PCANet: A simple deep learning baseline for image classification?" *IEEE Trans. Image Process.*, **24**, 5017–5032, (2015).

[16] Q. Du, H. Yang, "Similarity-based unsupervised band selection for hyperspectral image analysis," *IEEE Geosci. Remote Sens. Lett.*, **5**, 564–568, (2008).

[17] T. Ojala et al., "Multiresolution gray-scale and rotation invariant texture classification with local binary pattern," *IEEE Trans. Pattern Analysis Mach. Intell.*, **24**, 971–987, (2002).

[18] F. Melgani, L. Bruzzone, "Classification of hyperspectral remote sensing images with support vector machines," *IEEE Trans. Geosci. Remote Sens*., 42, 1778–1790, (2004).

[19] G. B. Huang, "An insight into extreme learning machines: random neurons, random forests and kernels," Cognitive Computation, **6**, 376–390, (2014).

[20] W. Li, C. Chen, H. Su, Q. Du, "Local binary patterns and extreme learning machines for hyperspectral imagery classification," **53**, 3681–3693, (2015).